Metrol. Meas. Syst., Vol. 31 (2024) No. 4, pp. 849–862
DOI: 10.24425/mms.2024.152055

PAN POLSKA AKADEMIA NAUK

METROLOGY AND MEASUREMENT SYSTEMS
Index 330930, ISSN 0860-8229
www.metrology.wat.edu.pl

M&MS

ALGORITHM FOR COMPENSATION OF EXTERNAL INFLUENCES UPON METAL OXIDE GAS SENSORS USING THE DATASHEET CHARACTERISTICS

Cristian Fosalau, Doru Cornei, Cristian Zet

Gheorghe Asachi Technical University of Iasi, Faculty of Electrical Engineering, Iasi, Romania
(✉ *cfosalau@tuiasi.ro*)

Abstract

Gas sensors, like any other type of sensors, are affected by external influencing factors among which the most aggressive are the ambient temperature and humidity. If the influence is small, their effect on the global accuracy of the sensor is reduced, and the error caused by these factors is included in the admissible error provided in the datasheet. However, if the influence ais significant, their effect can no longer be neglected and compensation of these errors is necessary based on the known influence characteristics found in the datasheet of the sensor. Unfortunately, these characteristics are not linear and the compensation must be accomplished according to an analytical relationship, if it can be known, or based on look-up tables implemented in the memory of the measuring device. Things get complicated when there are several influence factors. The paper describes a method for compensating the influence of ambient temperature and humidity on an MQ7 metal oxide gas (MOG) sensor, mainly dedicated to measuring carbon monoxide (CO), by mathematically modelling the surfaces of the characteristics given in the sensor's datasheet and their implementation on a microcontroller platform. Experimental data show that, for a temperature variation between 10 and 50 Celsius degrees (°C) and a relative humidity (RH) variation between 30 and 90%, a reduction of the total amount of error is obtained by compensating the influence quantities resulting in an accuracy improvement of more than 60%.

Keywords: metal oxide gas sensor, external factors influence compensation, datasheet, enhanced accuracy.

1. Introduction

In the context of the actual climate change, the problem of finding the values of the concentration of pollutant gas spread over large areas of land and in very different environmental conditions is becoming more and more of interest. Among the most used methods of monitoring of gases in the environment are those with measuring instruments that use sensors. There are numerous types of gas sensors with which gas analysers are equipped, both fixed and portable, operating according to several physicochemical principles. The technologies available to support gas sensors have rapidly advanced in the last decades. Some examples of such operating principles are given

Article history: received July 2, 2024; revised August 12, 2024; accepted August 27, 2024; available online November 6, 2024.

below. Solid electrolyte gas sensors [1], utilize as sensing material certain ionic crystals such as ZrO2 through which ionic current is established in the presence of a gas at high temperatures. Two principal designs are available in this case: potentiometric and amperometric. Capacitive gas sensors [2] can use as a principle the variations of the capacitance of a material due to either a change of the dielectric constant or a change in the thickness of the active layer produced by the gas to be detected. Calorimetric gas sensors [3] can detect changes of the temperature of the active surface layer, due to the adsorption of combustible gas molecules at the surface layer.

Gravimetric gas sensors can be found in two main designs, namely as *quartz crystal microbalance* (QCM) sensors [4] and as *surface acoustic wave* (SAW) detectors [5]. Both modes of operation are based on detecting changes of sensing layer mass owing to adsorption of gas molecules down to a nanogram by means of sensing variations of proper resonant frequency of the device. The operation of *infrared* (IR) spectroscopy optical sensors [6] is based on the interaction between the photons and the gas molecules which leads to a high degree of radiation adsorption in a very narrow range of frequencies and hence to a very good selectivity and sensitivity down to parts per billion (ppb) levels. Finally, there also exists a number of researches for sensors based on nanotechnologies in which the surface contact of the sensitive material with the gas is significantly increased and so is the device sensitivity [7]. However, the most utilized sensors in common instrumentation devoted to detecting and measuring gaseous pollutants, especially at emission sources, are those using metal oxide semiconducting materials as the functional layer. At higher temperatures, usually more than 300°C, the conductivity of these materials changes with the gas concentration due to the adsorption of gas molecules by the oxygen ions found at the surface layer [8, 9]. Their main advantages are the low cost and flexibility in production, the wide range of gases that can be detected, and simplicity of construction. However, they also exhibit important drawbacks such as low selectivity and sensitivity, high power consumption and strong susceptibility to external environmental influence factors e.g. ambient temperature and humidity. These two factors of influence seriously affect the device accuracy and, without appropriate measures of compensation, the measurement errors may rise in certain circumstances to more than 50%.

There are two ways of compensating temperature and/or humidity influence. One is based on well-known hardware methods, which include the bridge method, the negative temperature coefficient platinum resistance method and various configurations using operational amplifiers for signal conditioning. The other is based on software methods that are the most widely used in modern digitally oriented devices. Many approaches solve this problem by using *Machine Learning* (ML) algorithms. For example, [10] presents a solution for compensating systematic errors caused by temperature and humidity variations for a *Volatile Organic Compounds* (VOC) sensor using artificial neural networks. It turns out that the method is effective, but to calculate compensation, it is necessary to use significant resources capable of implementing the algorithm. In [11], a similar approach for compensating the influence errors for CO, NO_2, SO_2, O_3 and CO_2 gases using several Machine Learning algorithms such as Linear, Quadratic and Gaussian Regression Models, the Clustering Model and the Artificial Neural Network is presented and discussed. Also in these cases, the efficiency of the methods is good, but they have some limits for practical implementation. In other cases, the correction is modelled as an analytical relation to be implemented in the computing unit which drives the device, when the sensor characteristic must be known in advance. They are usually traced using relatively complicated and expensive experimental setups [12–14].

In this paper, a general method for improving the accuracy of a MOG sensor by mathematically modelling its behaviour under the influence of ambient temperature and humidity is presented. It will be shown that applying this method leads to diminishing the unfavourable influence of temperature and humidity more than eight times in certain circumstances. The theoretical development of the model and its experimental validation is provided for a particular MOG sensor

Metrol. Meas. Syst., Vol. 31 (2024), No. 4, pp. 849–862
DOI: 10.24425/mms.2024.152055

of the MQ7 type which is designed to sense *carbon monoxide* (CO), but the method may be successfully applied to other MOG sensors such as MQ2, MQ3, MQ4, MQ5, MQ6, MQ135, sensitive to smoke, alcohol, hydrogen, methane or ammonia, whose working principle is similar to that of MQ7. By extension, the procedure may also be applied to any sensor whose characteristics are significantly affected by external quantities provided that the influence characteristics are given in the datasheet or experimentally traced. An assessment of the algorithm's efficiency in terms of error reduction is finally discussed.

Compared to other methods found in the literature, mainly those comprising machine learning algorithms that offer the best performance but require high computing resources, the main merit of this method is that it provides a simple and affordable solution to improve the performances of a device equipped with a low-cost gas sensor by easy implementation in a process controller without requiring a large amount of processing resources, thus leading to a reduced cost of the equipment combined with obtaining adequate performances. The obtained performances are not spectacular, but they offer a very practical way of obtaining a reliable device with satisfactory qualities at a low price.

2. Proposed compensation algorithm

This section aims of to describe a method by which the measured value of gas concentration can be corrected in order to obtain a better accuracy of measurement when functioning under significant variations of conditions of ambient temperature and humidity.

2.1. Operating principle of the sensor

The operating principle of a MOG sensor is based on the oxidation-reduction reaction of the gas to be detected with the oxygen disposed on the surface of the sensitive surface of a metal oxide. As a result of this reaction, the conductivity and, finally, the electrical resistance of the material change with the gas concentration [8]. A scheme of this principle is given in Fig. 1, customized for *carbon monoxide* (CO). In the absence of CO, the interaction between atmospheric oxygen and

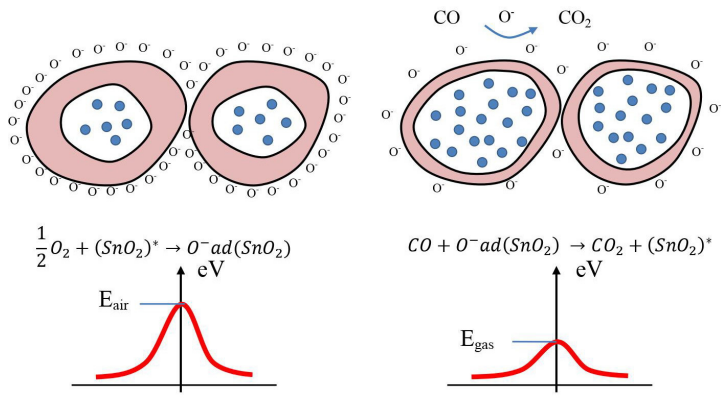

Fig. 1. Operating principle of a metal oxide gas sensor. Representation of two in-contact metal oxide grains in the absence of the sensing gas (left) when the potential barrier is high and so the material resistivity and in the presence of the sensing gas (right) when the potential barrier decreases.

the metallic oxide surface creates a potential barrier at the oxide grain boundary, which traps the electrons from the bulk of the material and thus its electrical resistivity becomes high.

In a CO gas atmosphere and at material temperatures of 300–400°C, the CO molecules are adsorbed on the oxide surface and recombine with the oxygen ions forming carbon dioxide CO_2, thus releasing the electrons from the trapping layer and decreasing the potential barrier. In this way, the electrical resistance decreases depending on the gas concentration. For N-type oxides (TiO_2, Nb_2O_5, Ta_2O_5, ZnO, SnO_2), conductivity increases, and hence the material resistance decreases in the presence of reducing gas, whereas for P-type oxides (NiO, CuO, Cr_2O_3, Co_3O_4), the things will happen conversely. Next, the presentation will be customized for an MQ7 type low-cost commercial sensor.

MQ7 is a sensor mainly dedicated to the detection and measurement of CO, but, like almost all MOG sensors, it is not selective, being to a lesser extent sensitive to other gases as well. In Fig. 2, the characteristics of MQ7 taken from its datasheet are given [16]. They represent the dependence of the ratio R_s/R_0 on the gas concentration C, where R_s is the sensor resistance at concentration C and R_0 is the sensor resistance at a reference concentration C_0 = 100 ppm CO. These characteristics are determined at typical external influences of temperature θ_0 = 20°C and relative humidity RH_0 = 33%. The sensor's sensitivity to other gases such as hydrogen (H_2), *liquid petroleum gas* (LPG) or methane (CH_4) can be also observed from the characteristics.

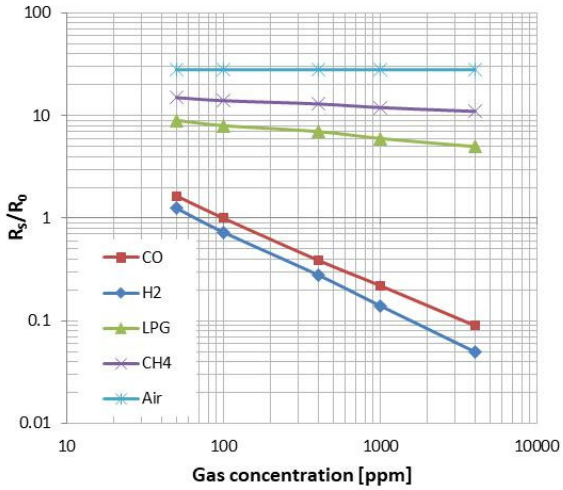

Fig. 2. Characteristics of the MQ7 sensor as in the datasheet [16]

The way the sensor is connected in an electrical circuit is depicted in Fig. 3a. As it can be noticed, the sensor contains four terminals: two of them through which the sensitive material is heated at temperatures of 300°C to 400 °C, whereas from the other two, the variable resistance R_s of the sensor is available. The sensor is electrically connected in the circuit through a voltage divider together with the load resistance R_L, from which the voltage V_m is measured. The supply voltage of the divider is V_s. The load resistance, R_L has a fixed value of about 10 kΩ, as indicated by the manufacturer. For ease of use, the sensor is available in a shield compatible with Arduino or ESP32 development boards, as shown in Fig. 3b.

Metrol. Meas. Syst., Vol. 31 (2024), No. 4, pp. 849–862
DOI: 10.24425/mms.2024.152055

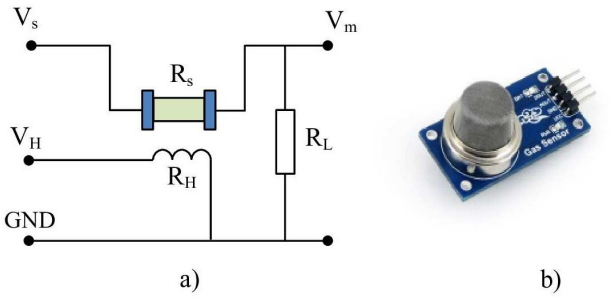

Fig. 3. a) Electrical circuit connection of the sensor, b) Arduino MQ7 shield [16].

2.2. Sensor scaling

Sensor scaling means finding the dependence of the gas concentration C on the measured voltage V_m picked from the voltage divider, that is:

$$C = \xi(V_m) \tag{1}$$

In Fig. 4 is given the dependence of the ratio R_s/R_0 on temperature for a range between -10°C and 50°C and for two different values of humidity, where R_0 is the sensor resistance at the reference concentration $C_0 = 100$ ppm CO, $\theta_0 = 20$°C and $\mathrm{RH}_0 = 33\%$, for which the ratio $R_s/R_0 = 1$.

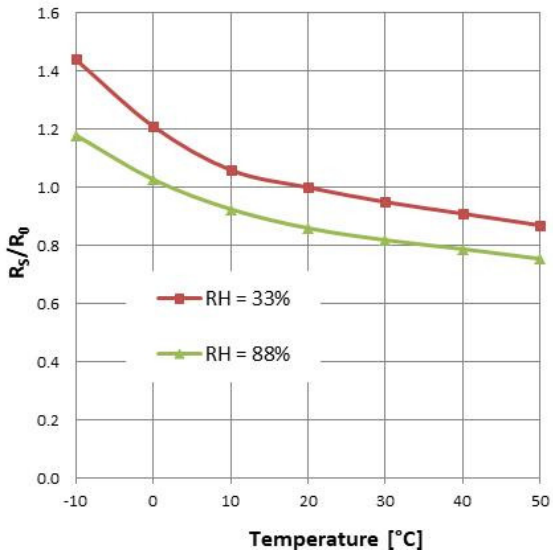

Fig. 4. Dependence of the sensor characteristics on temperature and humidity [10]].

First, the dependence of (1) for the reference conditions $\theta_0 = 20$°C and $\mathrm{RH}_0 = 33\%$ will be determined. For this, the characteristic given for the CO gas in Fig. 2 will be employed. One can observe here that this characteristic is fairly linear in logarithmic axes and may be approximated as:

$$\lg\left(\frac{R_s}{R_0}\right) = m \lg C + k \tag{2}$$

where m and k are the slope and the intercept of the line that may be calculated knowing the coordinates of two points on the characteristic. Let these two points be

$$A\left(x_1 = C_1, y_1 = \left(\frac{R_s}{R_0}\right)_1\right) \quad \text{and} \quad B\left(x_2 = C_2, y_2 = \left(\frac{R_s}{R_0}\right)_2\right). \tag{3}$$

Taking into account (1), it gives:

$$m = \frac{\lg y_1 - \lg y_2}{\lg x_1 - \lg x_2} = \frac{\lg\left(\frac{y_1}{y_2}\right)}{\lg\left(\frac{x_1}{x_2}\right)} \tag{4}$$

and

$$k = \frac{\lg x_1 \lg y_2 - \lg x_2 \lg y_1}{\lg x_1 - \lg x_2} \tag{5}$$

On the other hand, the voltage picked from the voltage divider, V_m, depends on the two resistances, R_s and R_L according to:

$$V_m = V_a \frac{R_L}{R_L + R_s} \Rightarrow R_s = R_L \frac{V_a - V_m}{V_m} \Rightarrow \frac{R_s}{R_0} = R_L\left(\frac{V_a}{V_m} - 1\right) \tag{6}$$

By applying the logarithm operation on (6), one obtains:

$$\lg\left(\frac{R_s}{R_0}\right) = \lg\left[R_L\left(\frac{V_a}{V_m} - 1\right)\right] = m \cdot \lg C + k. \tag{7}$$

From (6) and (7) one obtains the scaling equation which gives the dependence of the concentration C on the measured voltage, V_m, for temperature θ_0 and relative humidity RH_0:

$$C_{\theta_0,\mathrm{RH}_0} = 10^{\frac{1}{m}\left[\lg\left(\frac{R_s}{R_0}\right)_{\theta_0,\mathrm{RH}_0} - k\right]} = 10^{\frac{1}{m}\left[\lg\left[\frac{R_L}{R_0}\left(\frac{V_a}{V_m}-1\right)\right] - k\right]}. \tag{8}$$

The scaling equation may be computed using the microcontroller of the platform the system is deployed on.

2.3. External influences compensation algorithm

As stated before, according to the datasheet and experimental tests, metal oxide sensors, and in particular the MQ7 CO sensor, are strongly influenced by external parameters such as ambient temperature and humidity. The graphs in Fig. 2 represent the dependences of the ratio R_s/R_0 on gas concentration for $\theta_0 = 20°\mathrm{C}$ and $\mathrm{RH}_0 = 33\%$ where R_0 is the resistance of the sensor for $C = 100$ ppm CO. For these values, $\left(\frac{R_s}{R_0}\right)_{\theta_0,\mathrm{RH}_0}^{100\ \mathrm{ppm}} = 1$. Any deviation of θ and RH from the above values produces a change in the ratio R_s/R_0 by a value $\left(\frac{\Delta R_S}{R_0}\right)_{\theta,\mathrm{RH}}$ which will be called further on *correction* (Corr). Consequently, for a certain value of the concentration C, the corrected value of R_s/R_0 ratio at temperature θ and relative humidity RH will be given by:

$$\left(\frac{R_s}{R_0}\right)_{\theta,\mathrm{RH}}^{C} = \left(\frac{R_s}{R_0}\right)_{\theta_0,\mathrm{RH}_0}^{C} + \left(\frac{\Delta R_s}{R_0}\right)_{\theta_0,\mathrm{RH}_0}^{C}. \tag{9}$$

For ease of calculation and due to lack of sufficient information in the datasheet, the same correction over the entire measuring range of the sensor is assumed, i.e.:

$$\text{Corr} = \left(\frac{\Delta R_s}{R_0}\right)^{C}_{\theta_0,\text{RH}_0} = \left(\frac{\Delta R_s}{R_0}\right)^{100\,\text{ppm}}_{\theta_0,\text{RH}_0}. \tag{10}$$

With this simplification, one can calculate the corrected value of the measured ratio R_s/R_0 at any θ and RH for C0 = 100 ppm from the datasheet characteristics as:

$$\left(\frac{R_s}{R_0}\right)^{100\,\text{ppm}}_{\theta,\text{RH}} = \left(\frac{R_s}{R_0}\right)^{100\,\text{ppm}}_{\theta_0,\text{RH}_0} + \text{Corr} = 1 + \left(\frac{\Delta R_s}{R_0}\right)^{100\,\text{ppm}}_{\theta_0,\text{RH}_0}. \tag{11}$$

The quantity

$$\left(\frac{R_s}{R_0}\right)^{100\,\text{ppm}}_{\theta,\text{RH}} = f(\theta,\text{RH})$$

represents families of characteristics that describe a surface having θ and RH as variables. To determine this surface, the dependence $R_s/R_0 = f(\theta)$ will be first modelled by 3-order polynomials, obtaining:

$$\left(\frac{R_s}{R_0}\right)^{100\,\text{ppm}}_{\theta,\text{RH}} = a(\text{RH})\theta^3 + b(\text{RH})\theta^2 + c(\text{RH})\theta + d(\text{RH}) = P(\theta,\text{RH}) \tag{12}$$

Thus,

$$\text{Corr} = \left(\frac{\Delta R_s}{R_0}\right)^{100\,\text{ppm}}_{\theta_0,\text{RH}_0} = P(\theta,\text{RH}) - 1 \tag{13}$$

Since the characteristics in the sensor datasheet do not provide enough information regarding the variation with humidity apart from the dependencies for RH = 33% and RH = 88%, one may assume that the coefficients a(RH), b(RH), c(RH) and d(RH) have a linear variation with RH. By performing the linear fit of the four coefficients with RH, one obtains the following set of equations:

$$\begin{aligned} a(\text{RH}) &= m_a\text{RH} + k_a; \qquad & b(\text{RH}) &= m_b\text{RH} + k_b, \\ c(\text{RH}) &= m_c\text{RH} + k_c; \qquad & d(\text{RH}) &= m_d\text{RH} + k_d. \end{aligned} \tag{14}$$

On the other hand, the ratio correction *Corr* corresponds to the correction ΔV_m of the voltage measured under the same temperature and humidity conditions. By differentiating (7) one obtains

$$\left(\frac{\Delta R_s}{R_0}\right)^{100\,\text{ppm}}_{\theta_0,\text{RH}_0} = \frac{\partial\left[\frac{R_L}{R_0}\left(\frac{V_a}{V_m}-1\right)\right]}{\partial V_m}\Delta V_m = -\frac{\frac{R_L V_a}{R_0}}{V_m^2}\Delta V_m \tag{15}$$

from which the ΔV_m correction results as

$$\Delta V_m = -\frac{R_0}{R_L V_a}V_m^2\left(\frac{\Delta R_s}{R_0}\right)^{100\,\text{ppm}}_{\theta_0,\text{RH}_0}. \tag{16}$$

Finally, the corrected value of the measured voltage V_m will be:

$$(V_m)_c = V_m + \Delta V_m. \tag{17}$$

This value is introduced in (8) for finding the corrected concentration:

$$C_{\theta,\text{RH}} = 10^{\frac{1}{m}\left[\lg\left[\frac{R_L}{R_0}\left(\frac{V_a}{(V_m)_c}-1\right)\right]-k\right]}. \tag{18}$$

3. Experimental setup

In order to validate the proposed compensation algorithm, an experimental setup was built with which gas concentrations measured in different controlled environmental conditions using a commercially available MQ7 CO sensor were compared with reference concentrations of standard gas. The testing of the method was carried out for a single sensor, even if, for the correctness of the conclusions, the measurements should have been performed on larger, statistically significant batches of sensors. Because of this, the evaluation of the accuracy of the method is approximate, the intention of the paper being to provide a possible solution to improve the quality of the data measured with such sensors at a price as low as possible.

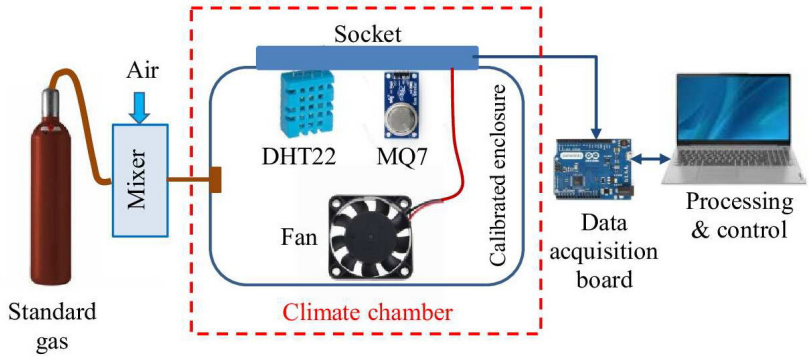

Fig. 5. Scheme of the experimental setup.

The experimental setup, schematically presented in Fig. 5, includes a sealed Plexiglas enclosure with a volume of 3.52 dm^3 equipped with a homogenization fan, in which the MQ7 sensor mounted in an Arduino-compatible shield is inserted. In the same enclosure, a DHT22 temperature and humidity sensor is also present with the aim to measure the two quantities at the same time with the gas concentration. DHT22 measures temperature with an accuracy of ±0.5°C and humidity within ±2% RH. The standard concentrations of CO were prepared by mixing pure CO with fresh air in various volumes. The pure gas is extracted from a gas cylinder of 99.7% purity acquired from Fluka. The signal produced by the sensor, namely the V_m voltage picked from the voltage divider $R_s - R_L$, as well as the signals delivered by the DHT22 sensor are acquired with an Arduino Leonardo compatible with MQ7 and DHT22 modules, whose role is to read the analogue signals, digitize them and transmit to a computer in which there runs a signal acquisition and processing virtual instrument built in LabVIEW. This software implements the relation (18) with which the corrected value of the concentration is calculated. In order to test the algorithm efficiency at different temperatures and *humidity values*, the Plexiglas enclosure was introduced in a Binder Model KBF P 240 constant climate chamber that can maintain constant inside both temperature and humidity in a range of 0 to 70°C and 10 to 90% RH respectively within an accuracy of 1.5%. A picture of the stand is given in Fig. 6. The maximum preparation error of standard concentrations is 0.76%.

Metrol. Meas. Syst., Vol. 31 (2024), No. 4, pp. 849–862
DOI: 10.24425/mms.2024.152055

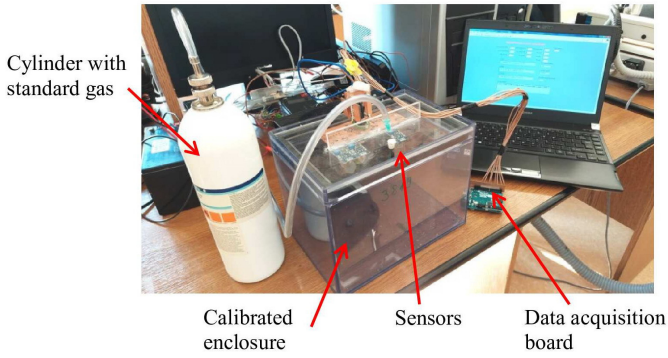

Fig. 6. View of the experimental setup.

4. Results and discussion

In this section, the evolution of voltage correction according to the mathematical model is accomplished by simulation, after which the experimental data are processed in order to draw a conclusion regarding the efficiency of the algorithm to reduce the external influences upon the results of measurement.

4.1. Simulation

In Fig. 7, the sensor characteristic meaning the dependence $C = \xi(V_m)$ calculated using (8) at particular conditions $C_0 = 100$ ppm CO, $R_s = 15$ kΩ, $R_L = 10$ kΩ and $V_s = 5$ V is given. A strong nonlinearity of the device can be noticed, which may limit its range of use.

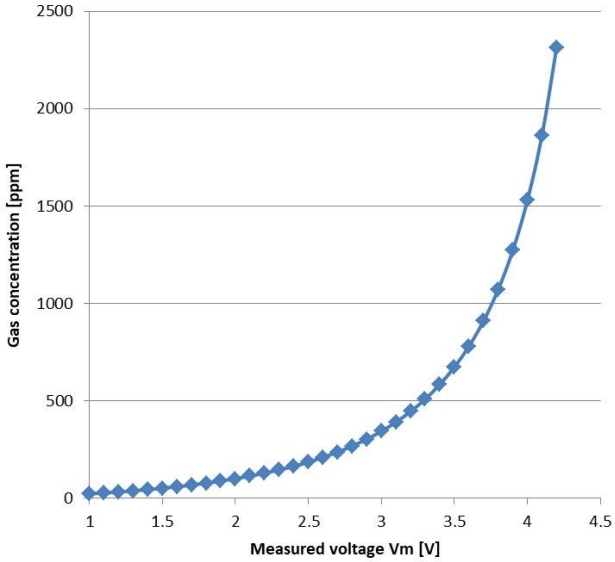

Fig. 7. Sensor characteristic representing the dependence $C = \xi(V_m)$.

In Fig. 8, the surface representing the dependence of the correction *Corr* on the two influence factors is computed according to (13). As stated earlier, *Corr* is considered constant over the whole sensor measurement range, at least in the range of 100 to 1500 ppm, in which the algorithm has been tested. This quantity is added to the actual measured value of gas concentration in order to obtain the corrected value as close to the standard concentration as possible.

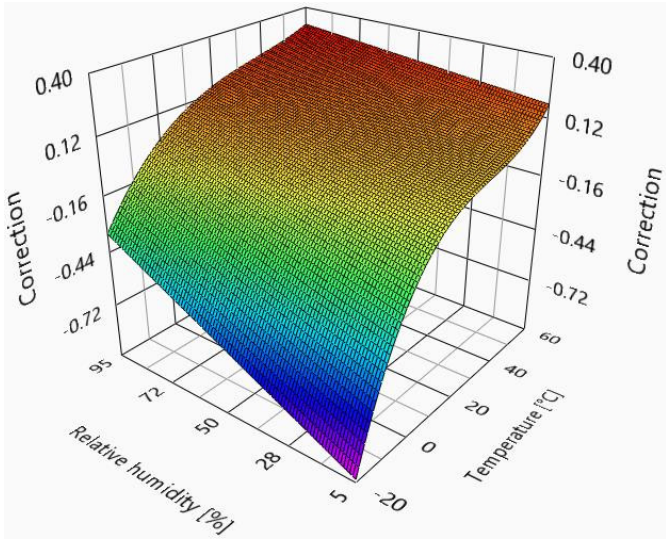

Fig. 8. Evolution of the correction factor *Corr* with respect to temperature and relative humidity simulated on the basis of (13).

4.2. Experimental data

In order to obtain experimental data using the above-described setup, the following steps have been carried out:

1. Sensor formatting, that is supplying the sensor with a voltage of 5 V for 24 hours, as indicated by the manufacturer in the datasheet;
2. Measuring the sensor resistance at reference conditions. The found value is $R_s = 14.7$ kΩ.
3. Adjusting the load resistance R_L so as to obtain the same reference value for concentration $C_0 = 100$ ppm in both corrected and uncorrected cases. The value is $R_L = 11.2$ kΩ.
4. Tracing the dependence $C_{\text{mas}} = f(C_{\text{standard}})$ in the concentration range between 100 ppm and 1300 ppm in steps of 200 ppm for different temperature and humidity conditions, including the reference conditions.
5. Calculating the relative errors and interpreting the results.

The method was tested using an ATMega32U4 microcontroller on the Arduino Leonardo platform employed as an acquisition and computing unit. Compared with the response time of the concentration variation (order of seconds), the acquisition and calculation times of the correction are insignificant. One of the board's analogue inputs was used to acquire the voltage provided by the MQ7 sensor, whereas the communication with the DHT22 sensor was realised through the one-wire interface. The entire program implemented on the microcontroller occupied 12.7 kB of memory.

Metrol. Meas. Syst., Vol. 31 (2024), No. 4, pp. 849–862
DOI: 10.24425/mms.2024.152055

In order to assess the efficiency of the proposed method, the relative errors obtained for corrected and uncorrected values have been calculated according to the formulas:

$$e_{\text{corr}} = \max\left[\frac{|C_s - C_{\text{corr}}|}{C_s}100\right] \tag{19}$$

and

$$e_{\text{uncorr}} = \max\left[\frac{|C_s - C_{\text{uncorr}}|}{C_s}100\right], \tag{20}$$

where e_{corr} and e_{uncorr} are the maximum relative errors in corrected and uncorrected cases respectively, C_s is the standard value of gas concentration at every point of the characteristic, and C_{corr} and C_{uncorr} are the values computed with (8) and (18) respectively. The errors above were calculated without considering the accuracy of the standard concentration set for every point of the characteristic, as it remained the same for all testing points.

In Fig. 9a) to d), the evolution of the measured corrected and uncorrected values of gas concentration is traced with respect to standard concentrations known within the accuracy of 0.76% and different ambient conditions of temperature and humidity. In these plots, the first bisector has been also traced, taking it as a reference, because it represents the true values of gas concentration.

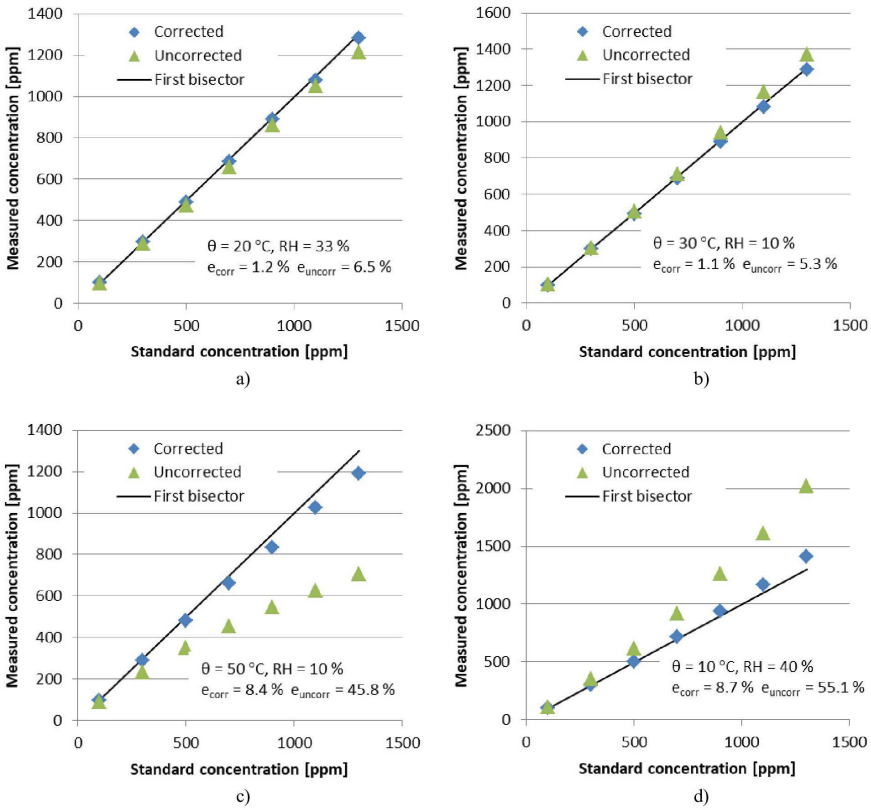

Fig. 9. Dependence of corrected and uncorrected measured values of gas concentration on standard concentrations for different values of temperature θ and relative humidity RH. For every case, the maximum relative errors are specified.

4.3. Discussion

As it can be observed at first glance from Fig. 9, the corrected values are much closer to the first bisector than the uncorrected ones, meaning that the errors are relatively small for these characteristics. The uncorrected characteristics have very large deviations from the first bisector in certain situations. These deviations may be above or below the first bisector. In Table 1, the calculated values of the maximum relative errors are given for the experimental data in various combinations. Analysing these results, one can notice that there exists a significant difference between the errors obtained for corrected measurements and the uncorrected ones, from which the overall conclusion can be drawn that the algorithm works well in some situations, especially when the influence conditions are extreme.

Table 1. Calculated maximal relative errors for different experimental data.

θ [°C]	RH [%]	Maximum relative error e [%]	
		Corrected	*Uncorrected*
20	33	1.2	6.5
30	10	1.1	5.3
50	10	8.4	45.8
10	40	8.7	55.1
30	70	9.8	57.3
50	90	9.9	58.4

One can also observe that even the corrected values are affected by errors and that they increase to the higher end of the tested range. These errors may have multiple causes such as imprecision of voltage readings with the microcontroller, technological dispersion of MQ7 sensor characteristics, imprecision in reading the temperature and humidity with DHT22, assumption that the correction is constant over the whole range, uncorrected approximation of the surface, *etc*.

5. Conclusions

In the paper, a method for improving the low-cost metal oxide gas sensors performance based on a mathematical model developed starting from the datasheet characteristics is presented. The model can be implemented as a computer algorithm on a digital platform or a microcontroller. By experimental trials, it has been proved that the measurement accuracy can be improved by lowering the influence of external factors such as temperature and humidity, especially when their values are extreme. The maximum experimental error resulting from the performed tests with the correction applied is less than 10 %, whereas without correction, the error may augment to more than 55 %. The main benefit of this method is that the compensation relation can be deduced from the very datasheet characteristics and it can be easily deployed on computing units with limited resources, leading to a significant improvement in measurement accuracy. It is also important to note that the method can be utilized and implemented for compensating the errors of any other sensor or device prone to large influence of external factors.

References

[1] Ritter, T., Zosel, J., & Guth, U. (2023). Solid electrolyte gas sensors based on mixed potential principle – A review. *Sensors and Actuators B: Chemical*, *382*, 133508. https://doi.org/10.1016/j.snb.2023.133508

[2] Yu, H., Sun, A., Liu, Y., Zhou, Y., Fan, P., Luo, J., Zhong, A. (2021). Capacitive sensor based on GaN honeycomb nanonetwork for ultrafast and low temperature hydrogen gas detection, *Sensors and Actuators B: Chemical, Vol. 346*, 130488. https://doi.org/10.1016/j.snb.2021.130488

[3] N.-H. Park, N.H., Akamatsu, T., Itoh, T., Izu, N., Shin, W., (2014). Calorimetric Thermoelectric Gas Sensor for the Detection of Hydrogen, Methane and Mixed Gases. *Sensors, 14(5),* 8350-8362. https://doi.org/10.3390/s140508350

[4] Quang, V.V., Hung, V.N., Tuan, L.A., Phan, V.N., Huy, T.Q., & Quy, N.V. (2014). Graphene-coated quartz crystal microbalance for detection of volatile organic compounds at room temperature. *Thin Solid Films*, *568*, 6–12. https://doi.org/10.1016/j.tsf.2014.07.036

[5] Guz, Ł. (2019). Technical aspects of SAW gas sensors application in environmental measurements. *MATEC Web of Conferences*, *252*, 06007. https://doi.org/10.1051/matecconf/201925206007

[6] Bogue, R. (2015). Detecting gases with light: a review of optical gas sensor technologies. *Sensor Review*, *35*(2), 133–140. https://doi.org/10.1108/sr-09-2014-696

[7] Abideen, Z.U., Kim, J.-H., Lee, J.-H., Kim, J.-Y., Mirzaei, A., Kim, H.W., & Kim, S. S. (2017). Electrospun Metal Oxide Composite Nanofibers Gas Sensors: A Review. *Journal of the Korean Ceramic Society*, *54*(5), 366–379. https://doi.org/10.4191/kcers.2017.54.5.12

[8] Dey, A. (2018). Semiconductor metal oxide gas sensors: A review. *Materials Science and Engineering: B*, *229*, 206–217. https://doi.org/10.1016/j.mseb.2017.12.036

[9] Wang, C., Yin, L., Zhang, L., Xiang, D., & Gao, R. (2010). Metal Oxide Gas Sensors: Sensitivity and Influencing Factors. *Sensors*, *10*(3), 2088–2106. https://doi.org/10.3390/s100302088

[10] Hajmirzaheydarali, M., & Ghafarinia, V. (2011). A Smart Gas Sensor Insensitive to Humidity and Temperature Variations. *IOP Conference Series: Materials Science and Engineering*, *17*, 012047. https://doi.org/10.1088/1757-899x/17/1/012047

[11] Malings, C., Tanzer, R., Hauryliuk, A., Kumar, S.P.N., Zimmerman, N., Kara, L. B., & Presto, A.A. (2019). Development of a general calibration model and long-term performance evaluation of low-cost sensors for air pollutant gas monitoring. *Atmospheric Measurement Techniques*, *12*(2), 903–920. https://doi.org/10.5194/amt-12-903-2019

[12] Gamboa, V.S., Kinast, É.J., & Pires, M. (2023). System for performance evaluation and calibration of low-cost gas sensors applied to air quality monitoring. *Atmospheric Pollution Research*, *14*(2), 101645. https://doi.org/10.1016/j.apr.2022.101645

[13] Kang, Y., Aye, L., Ngo, T.D., & Zhou, J. (2022). Performance evaluation of low-cost air quality sensors: A review. *Science of The Total Environment*, *818*, 151769. https://doi.org/10.1016/j.scitotenv.2021.151769

[14] De Vito, L., Cocca, V., Riccio, M., & Tudosa, I. (2012). Wireless Active Guardrail System for environmental measurements. *2012 IEEE Workshop on Environmental Energy and Structural Monitoring Systems (EESMS)*, 50–57. https://doi.org/10.1109/eesms.2012.6348403

[15] Hanwey Electronics Co., *MQ7 Sensor Datasheet*. https://semiconductors.es/datasheet/MQ7.html

[16] MQ7 Arduino shield datasheet and application: https://www.arduino.cc/reference/en/libraries/mq7sensor

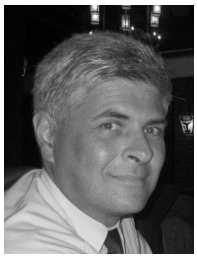

Cristian Fosalau received his Ph.D. in electrical engineering in 1998 from the Gheorghe Asachi Technical University of Iasi, Romania. He is now a full professor of electrical measurements, virtual instrumentation and signal processing at the Faculty of Electrical Engineering of the university. His research interests are focused on signal processing for instrumentation, virtual instrumentation, analogue and digital conditioning circuitry for sensors, sensitive elements based on nanotechnology, IoT systems for environment, agriculture and e-medicine, AI applied in measurement data processing. He is the author or co-author of over 130 papers published in indexed journals and conference proceedings.

Doru Cornei received his B.Sc. and M.Sc. diplomas from the Dunărea de Jos University of Galati, Romania, in 1996 and 1998 respectively. He is now a Ph.D. student in metrology and measurement systems at the Gheorghe Asachi Technical University of Iasi, Romania. He is an expert in analogue and digital electronics applied to signal acquisition and processing in large measurement distributed networks, as well as using programmable devices for process control. Since 2000, he has worked at the INFOSTAR Company Pascani as an electronic engineer.

Cristian Zet received his Ph.D. degree in electronics in 2002 from the Gheorghe Asachi Technical University of Iasi, Romania. He is currently a professor at the Department of Electrical Measurements, Faculty of Electrical Engineering at the same university. He is also employed at the Laboratory of Modern Measurements Systems. His research interests include sensors and transducers, data acquisition systems, analogue and digital signal processing and circuits, virtual instrumentation, programmable circuits and embedded systems.